

Ultrasound Attenuation of Superfluid ^3He in Aerogel

H.C. Choi, N. Masuhara, B.H. Moon, P. Bhupathi, M.W. Meisel, and Y. Lee*

Microkelvin Laboratory, Department of Physics, University of Florida, Gainesville, FL 32611-8440, USA

N. Mulders

Department of Physics and Astronomy, University of Delaware, Newark, DE 19716, USA

S. Higashitani, M. Miura, and K. Nagai

Faculty of IAS, Hiroshima University, Kagamiyama 1-7-1, Higashi-Hiroshima 739-8521, Japan

(Dated: February 8, 2022)

We have performed longitudinal ultrasound (9.5 MHz) attenuation measurements in the B-phase of superfluid ^3He in 98% porosity aerogel down to the zero temperature limit for a wide range of pressures at zero magnetic field. The absolute attenuation was determined by direct transmission of sound pulses. Compared to the bulk fluid, our results revealed a drastically different behavior in attenuation, which is consistent with theoretical accounts with gapless excitations and a collision drag effect.

Liquid ^3He has attracted intense interest for many decades in the field of low temperature physics [1]. In its normal state, liquid ^3He has served as a paradigm for a Fermi liquid whose nature transcends ^3He physics. The superfluid phases of ^3He exhibit exotic and intriguing features associated with the broken symmetries in the condensate, having an unconventional structure of the order parameter with spin triplet *p-wave* pairing. Liquid ^3He is arguably the most well-understood system mainly because of its extreme intrinsic purity at low temperatures. Therefore, it has provided important insights in understanding other unconventional superconductors such as the high temperature superconductors, the heavy fermion superconductors, and in particular the more recently discovered Sr_2RuO_4 , which is also thought to have the *p-wave* symmetry [2]. However, the same virtue has hampered the effort in pursuing answers to an important overarching question: how does the nature of a quantum condensate (spin triplet *p-wave* superfluid in this case) respond to increasing impurity or disorder?

Observation of superfluid transitions in liquid ^3He impregnated in high porosity aerogel in 1995 [3, 4] opened a novel path to introducing static disorder in liquid ^3He . Aerogel possesses a unique structure, whose topology is at the antipode of widely studied porous media such as Vycor glass and metallic sinters. Due to its open structure, there are no well-defined pores in aerogel and consequently, the liquid is in the proximity to the bulk. Ninety eight percent porosity aerogel, which has been used in most of the studies including this work, offers a correlated network of strand-like aggregates of SiO_2 molecules whose structure can be characterized by the geometrical mean free path ($\ell \simeq 100 - 200$ nm), the diameter of strand ($r \simeq 3$ nm), and the average inter-strand distance ($d \simeq 25 - 40$ nm). The coherence length of pure superfluid ^3He , ξ_0 , which varies from 20 nm (34 bar) to 80 nm (0 bar), is at least an order of magnitude larger than the strand diameter but is comparable to ℓ and d . As a result, the

scattering off the aerogel strand would have a significant influence on the superfluid. It is now well established that the superfluid transition temperature is significantly depressed from that of the bulk, and the effect of pair-breaking is progressively magnified at lower pressures, leading to the possibility of a quantum phase transition at $P_c \approx 6$ bars [5]. To date, three distinct superfluid phases have been experimentally identified, namely the A-like, B-like, and A_1 -like phases [4, 6, 7, 8, 9]. The B-like phase and the A_1 -like phase in aerogel show striking similarity to their counterparts in the bulk superfluid [9, 10]. Detailed NMR studies [7, 8, 10] suggest that the aerogel B-phase has the same order parameter structure as the bulk B-phase. The aerogel A_1 -phase only appears in the presence of magnetic field as is the case in the bulk [9]. However, the aerogel A-phase exhibits quite a different behavior from the bulk A-phase (*e.g.* in NMR frequency shift and superfluid density), although the overwhelming experimental evidence suggests that it is an equal spin pairing state. Various interpretations or novel propositions on the possible order parameter structure have been suggested for this phase [11, 12, 13].

Nuclear magnetic resonance and ultrasound spectroscopy have been used in concert to investigate the microscopic structure of the superfluid phases [1, 14]. These two experimental methods encompass complementary information on the orbital (ultrasound) and spin (NMR) structure of the Cooper pairs. Rich spectra of order parameter collective modes in bulk superfluids, which are the fingerprints of specific broken symmetries in the system, have been mapped by ultrasound spectroscopic techniques [14]. In 2000, Nomura *et al.* [15] performed ultrasound attenuation measurements on 98% aerogel using a 16.5 MHz cw acoustic impedance technique. Their work was limited to a single pressure at 16 bars and down to 0.6 mK. Although their technique was not adequate in determining absolute attenuation, they managed to extract the absolute sound attenuation after making auxil-

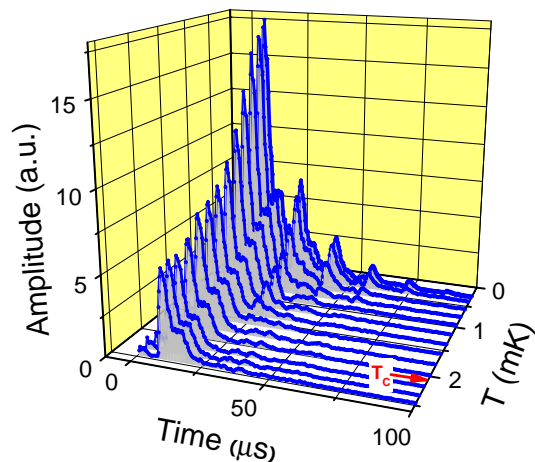


FIG. 1: Acoustic response from the receiver vs. time at 34 bars for select temperatures ranging from 0.3 mK to 2.5 mK. The aerogel superfluid transition is marked by a small arrow.

ary assumptions. A Bayreuth group [16] performed absolute sound attenuation measurements in aerogel (97% porosity) using a direct sound transmission technique at 10 MHz. They experienced poor transducer response, and observed self-heating and no depression in the aerogel superfluid transition. We conducted high frequency sound transmission experiments in 98% porosity aerogel, covering the whole phase diagram of the superfluid phases in aerogel, from 8 to 34 bars and from the transition temperatures to as low as 200 μK .

In this experiment, two matched LiNbO_3 longitudinal sound transducers with the fundamental resonance at 9.5 MHz were used as a transmitter and a receiver. The 6.3 mm diameter transducers were separated by a Macor spacer maintaining a $3.05 (\pm 0.02)$ mm sound path between the transducers where the aerogel sample was grown *in situ*. This scheme ensures the best contact between the transducer surface and the aerogel, which is crucial for clean sound transmission at the boundaries. A 1 μs pulse was generated by the transmitter and detected by the receiver. Temperature was determined by a melting pressure thermometer (MPT) for $T \geq 1$ mK and a Pt NMR thermometer for $T \leq 1$ mK which was calibrated against the MPT. No non-linear response or self-heating was observed at the excitation level used in this work. All the data presented here, except for 8 bars, were taken while warming with a typical warming rate of 3 $\mu\text{K}/\text{min}$. A detailed description on the experimental cell and experimental techniques can be found elsewhere [17, 18].

The temporal responses of the receiver taken at 34 bars are shown in Fig. 1 for select temperatures ranging from 0.3 to 2.5 mK. The primary response, which starts to rise around 8 μs , shows a rather broad response due to ringing of the high Q transducer ($Q \sim 10^3$). The step-like structure of the receiver signal is caused by the slight mis-

match in the spectra of the transducers [18]. Below the aerogel superfluid transition (marked around 2.1 mK by an arrow in Fig. 1) the primary response starts to grow and the trailing echoes emerge from the background, as the sound attenuation decreases in the superfluid. No change in the receiver signal was observed at the bulk superfluid transition. The multiple echoes follow a *bona fide* exponential decay in time. Absolute sound attenuation was obtained in the following manner [19]. First, the relative attenuation at each temperature was calculated using the area under the primary response curve by integrating the signal from the rising edge to a fixed point in time (23 μs point). The absolute attenuation at 0.4 mK and 29 bars, obtained using the primary signal and the echoes, was used as a reference point in converting the relative attenuation into the absolute attenuation. Due to a drastic mismatch in the acoustic impedance at the the transducer-aerogel/ ^3He boundary, the signal absorption at the surface of transducers was ignored [19]. The possible background contributions to attenuation from the quasi-particle scattering off the cavity wall [20] and the non-parallel alignment of the two transducers are estimated to be negligible.

The absolute attenuations on warming for several pressures are plotted as a function of temperature in Fig. 2(a). The superfluid transition is marked by the smooth drop in attenuation. Our aerogel superfluid transition temperatures are in excellent agreement with the previously reported values for all pressures [5, 21]. At 9.5 MHz in the *bulk* B-phase, a strong attenuation peak appears right below the superfluid transition. This peak is the result of the combined contributions from pair-breaking and coupling to the order parameter collective modes. Above the polycritical pressure, the B to A transition on warming is registered as a sharp step in attenuation. In *aerogel*, none of these features exist. However, we did observe a sharp step in attenuation on cooling for $P > 14$ bars, which implies the existence of the supercooled A-phase [19]. We were able to identify a rather smooth B to A transition on warming for 29 and 34 bars within ≈ 150 μK below the superfluid transition. This observation is consistent with the previous results obtained using a transverse impedance technique [13]. Therefore, most of the attenuation data presented here are in the aerogel B-phase. In the bulk B-phase with a clean gap, the attenuation follows $\alpha \propto e^{-\Delta(T)/k_B T}$ below the attenuation peak, practically reaching zero attenuation below $T/T_c \approx 0.6$, due to thermally activated quasi-particles, where $\Delta(T)$ is the temperature dependent gap and k_B is the Boltzmann constant. In contrast, the attenuation in aerogel decreases rather slowly with temperature and remains high even at $T/T_c \approx 0.2$. Furthermore, a peculiar shoulder feature appears at $T/T_c \approx 0.6$ for higher pressures. This feature weakens gradually and eventually disappears at lower pressures, Fig. 2(a).

Sound propagation for higher harmonics up to 96 MHz

was measured for several temperatures and pressures, but no evidence of sound propagation was found above 30 MHz even at 0.3 mK, where the lowest attenuation is expected. Below about 10 mK, the scattering process is dominated by the temperature independent impurity scattering off the aerogel, and at 9.5 MHz, $\omega\tau_i \sim 0.1$ for all pressures where $\tau_i = \ell/v_f$ (see below for ℓ). Therefore, the sound mode should remain in the hydrodynamic limit. This claim is bolstered by the observation of the strong frequency dependence in attenuation and the absence of a temperature dependence in the normal fluid attenuation [15]. The coupling between the normal component of the superfluid ^3He and the mass of the elastic aerogel modifies the conventional two-fluid hydrodynamic equations [22, 23]. This consideration leads to two (slow and fast) longitudinal sound modes with different sound speeds, $c_s = c_a \sqrt{\rho_s \rho_a / \rho}$, and $c_f = c_1 \sqrt{\frac{1 + \rho_a \rho_s / \rho_n \rho}{1 + \rho_a / \rho_n}}$. Here, $c_{f(s)}$ represents the speed of the fast (slow) mode, $\rho_{n(s)}$ is the normal fluid (superfluid) density ($\rho = \rho_n + \rho_s$), ρ_a is the aerogel density, c_1 is the speed of hydrodynamic sound in ^3He , and finally c_a is the sound speed of the bare aerogel. From the time of flight measurements, we found the sound speed in aerogel consistently lower (by $\approx 20\%$) than c_1 for all pressures studied and in good agreement with the values obtained using the expression above [24]. Detailed analysis of sound velocity for various pressures will be presented in a separate publication.

Low mass density and the compliant nature of aerogel necessitate the consideration of effective momentum transfer upon quasi-particle scattering off the aerogel, which generates dragged motion of aerogel. Ichikawa *et al.* [25] incorporated the collision drag effect in calculating the dispersion relation in the normal fluid. Their model offered a successful explanation for the experimental results of the Northwestern group [15]. Recently, Higashitani *et al.* [26, 27] extended this model to study the longitudinal sound (fast mode) propagation in superfluid ^3He /aerogel within the framework of the two-fluid model. The drag effect can be described phenomenologically by a frictional force, $\vec{F}_d = \frac{\rho_a}{\tau_f}(\vec{v}_n - \vec{v}_a)$, introducing an additional relaxation time τ_f , where $\vec{v}_{n(a)}$ is the normal fluid component (aerogel) velocity. This effect is of particular importance when $\omega\tau_i < 1$, and the total attenuation (Eq. (130) of ref. [27]) is

$$\alpha = \frac{\omega^2/2c_f}{1 + \rho_a \rho_s / \rho_n \rho} \left(\frac{\rho_a^2 \tau_f / \rho \rho_n}{1 + \rho_a / \rho_n} + \frac{4\eta/3\rho c_1^2}{1 + \rho_a \rho_s / \rho_n \rho} \right), \quad (1)$$

where η is the shear viscosity of liquid ^3He . The first term (α_f) arises from the frictional damping caused by the aerogel motion relative to the normal fluid component, and the second term (α_v) from the conventional hydrodynamic sound damping associated with the viscosity. This expression allows us to extract ℓ in this system from our absolute attenuation at the transition temperature, α_c . The inset of Fig. 3 shows our results of α_c for

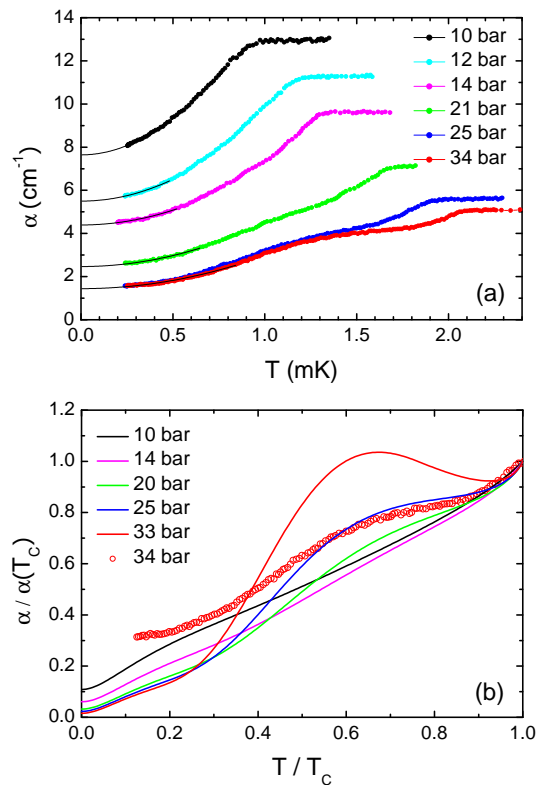


FIG. 2: (a) Absolute attenuation for various pressures vs. temperature (color in on-line version). Thin solid lines are the results of a quadratic fit to the low temperature part ($T/T_c \lesssim 0.4$) of the data at each pressure. (b) Normalized sound attenuation vs. normalized temperature. The results of theoretical calculation (solid lines, color in on-line version) are plotted along with the experimental results at 34 bars for comparison.

various pressures. The solid lines are the result of calculation using Eq. (1) for three different mean free paths, $\ell = 100, 120,$ and 140 nm. As can be seen, $\ell = 120$ nm produces an excellent fit to our data for the whole pressure range, which is in good agreement with the values obtained from the thermal conductivity (90 nm) [28] and spin diffusion (130 nm) [29] measurements. With the knowledge of the mean free path, one can calculate the full temperature dependence of sound attenuation in the superfluid phase. The results of the calculation (in the unitary limit) following the prescription described in ref. [27] are displayed in Fig. 2(b) along with the experimental results at 34 bars. The calculation reproduces all the important features observed in our measurements. In particular, the conspicuous shoulder structure appearing near $T/T_c \approx 0.6$ at 33 bars softens at lower pressures and is completely absorbed in an almost linear temperature dependence below 20 bars. This behavior is the characteristic of α_f [27]. A fast decrease in ρ_n right below T_c produces the bump in α_f , and $\alpha_f \rightarrow 0$ as $T \rightarrow 0$. On the other hand, α_v decreases monotonically and reaches a finite value due to non-zero ρ_n and the impurity states

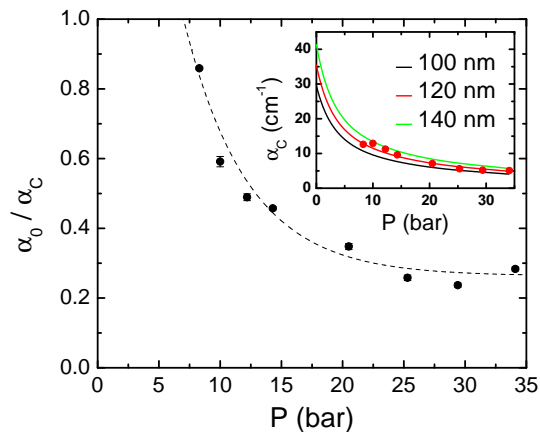


FIG. 3: Normalized zero temperature attenuation vs. pressure. The dashed line is a guide for eye. Inset: Pressure dependence of sound attenuation at T_c . The solid lines (color on-line) are the results of theoretical fit for $\ell = 100, 120,$ and 140 nm (see text).

induced inside the gap as $T \rightarrow 0$. The quantitative agreement between the theory and experiment, however, is not yet satisfactory. The calculation utilizes the isotropic homogeneous scattering model (IHSM) [30], which tends to overestimate $\Delta(T)$ and ρ_s compared to the experimentally determined values [3, 23]. As shown in ref. [31], the inhomogeneity gives rise to the reduction of the average value of the order parameter and consequently yields larger η and ρ_n , which in turn increases α_0 but decreases the frictional contribution. It is also expected that the non *s-wave* scattering components make non-trivial contributions to the viscous and frictional relaxation times in a direction that improves the quantitative agreement.

Theoretical calculations based on the IHSM [27, 32] predict that the impurity states would completely fill the gap, leading to a gapless superfluid when $\tau_i T_c < 1$ for the B-phase in the unitary limit. We estimate $0.3 < \tau_i T_c < 1$ for $10 < P < 34$ bars with $\ell = 120$ nm. The normalized zero temperature attenuation (α_0/α_c) obtained by extrapolating the low temperature part of the attenuation (solid lines in Fig. 2(a)) is plotted in Fig. 3, where α_0/α_c increases as the sample pressure is reduced and seems to approach unity near $P_c \approx 6$ bars. Since the viscosity ratio is directly related to the density of states at zero energy through $\eta(0)/\eta(T_c) = n(0)^z$, $z = \{2,4\}$ for the {Born, unitary} limit where $n(0)$ is the normalized density of states at zero energy [27], the finite α_0/α_c is strong evidence of a finite $n(0)$. The gapless behavior has been experimentally suggested by recent thermal conductivity (for $P \leq 10$ bars) [28] and heat capacity (for $11 \leq P \leq 29$ bars) [33] measurements. The pressure dependence of α_0/α_c is in qualitative agreement with the combined results of Fisher *et al.* and Choi *et al.* Although all of these experimental techniques (including ours) are limited to probe the impurity states near the Fermi level,

the behavior is consistent with the theoretical predictions with gapless excitations. Unlike the thermodynamic and transport measurements, the high frequency ultrasound measurement has a potential to unveil a larger portion of the impurity states profile from the frequency dependence.

We acknowledge support from an Alfred P. Sloan Research Fellowship (YL), NSF grants DMR-0239483 (YL), DMR-0305371 (MWM), and a Grant-in-Aid for Scientific Research on Priority Areas (No. 17071009) from MEXT of Japan (SH and KN). We would like to thank J.-H. Park for his technical assistance, and Jim Sauls, Peter Wölfle, and Bill Halperin for useful discussions.

* yoonslee@phys.ufl.edu

- [1] D. Vollhardt and P. Wölfle, *The Superfluid Phases of Helium Three*, (Taylor and Francis, London, 1990).
- [2] A.P. Mackenzie and Y. Maeno, *Rev. Mod. Phys.* **75**, 657 (2003).
- [3] J.V. Porto and J.M. Parpia, *Phys. Rev. Lett.* **74**, 4667 (1995).
- [4] D. T. Sprague *et al.*, *Phys. Rev. Lett.* **75**, 661 (1995).
- [5] K. Matsumoto *et al.*, *Phys. Rev. Lett.* **79**, 253 (1997).
- [6] D.T. Sprague *et al.*, *Phys. Rev. Lett.* **77**, 4568 (1996).
- [7] H. Alles *et al.*, *Phys. Rev. Lett.* **83**, 1367 (1999).
- [8] B.I. Barker *et al.*, *Phys. Rev. Lett.* **85**, 2140 (2000).
- [9] H.C. Choi *et al.*, *Phys. Rev. Lett.* **93**, 145302 (2004).
- [10] V.V. Dmitriev *et al.*, *JETP Lett.* **76**, 312 (2002); V.V. Dmitriev *et al.*, *Physica B* **329**, 324 (2003).
- [11] G.E. Volovik, *JETP Lett.* **63**, 301 (1996).
- [12] I.A. Fomin, *J. Low Temp. Phys.* **134**, 769 (2004).
- [13] C. L. Vicente *et al.*, *Phys. Rev. B* **72**, 094519 (2005).
- [14] W.P. Halperin and E. Varoquaux, in *Helium Three*, ed. by W.P. Halperin and L.P. Pitaevski (Elsevier, Amsterdam, 1990).
- [15] R. Nomura *et al.*, *Phys. Rev. Lett.* **85**, 4325 (2000).
- [16] L. Hristakos, Ph.D. thesis, University of Bayreuth (2001).
- [17] H.C. Choi *et al.*, will appear in *J. Low Temp. Phys.*
- [18] H.C. Choi, Ph.D. thesis, University of Florida (2007).
- [19] Y. Lee *et al.*, will appear in *J. Low Temp. Phys.*
- [20] G. Eska *et al.*, *Phys. Rev. B* **27**, 5534 (1983).
- [21] G. Gervais *et al.*, *Phys. Rev. B* **66**, 054528 (2002).
- [22] M.J. McKenna, T. Slawcki, and J.D. Maynard, *Phys. Rev. Lett.* **66**, 1878 (1991).
- [23] A. Golov *et al.* *Phys. Rev. Lett.* **82**, 3492 (1999).
- [24] For example, $c = 350 (\pm 10)$ m/s at 34 bars from our measurement, and $c_f = 370$ m/s.
- [25] T. Ichikawa *et al.*, *J. Phys. Soc. Jpn.* **70**, 3483 (2001).
- [26] M. Miura *et al.*, *J. Low Temp. Phys.* **134**, 843 (2004).
- [27] S. Higashitani *et al.*, *Phys. Rev. B* **71**, 134508 (2005).
- [28] S. N. Fisher *et al.*, *Phys. Rev. Lett.* **91**, 105303 (2003).
- [29] J.A. Sauls *et al.*, *Phys. Rev. B* **72**, 024507 (2005).
- [30] E. V. Thuneberg *et al.*, *Phys. Rev. Lett.* **80**, 2861 (1998).
- [31] R. Hänninen and E.V. Thuneberg, *Phys. Rev. B* **67**, 214507 (2003).
- [32] P. Sharma and J.A. Sauls, *Physica B* **329-333**, 313 (2003).
- [33] H. Choi *et al.*, *Phys. Rev. Lett.* **93**, 145301 (2004).